Langmuir

Article

pubs.acs.org/Langmuir

Hydrogelation Induced by Fmoc-Protected Peptidomimetics

Nicola Zanna, Andrea Merlettini, Giuseppina Tatulli, Lorenzo Milli, Maria Letizia Focarete,* and Claudia Tomasini*

Dipartimento di Chimica Ciamician, Università di Bologna, Via Selmi 2, 40126 Bologna, Italy

Supporting Information

ABSTRACT: Four new low molecular weight hydrogelators (LMWGs) have been prepared in multigram scale and their attitude to form hydrogels has been tested. The gelation trigger is pH variation. The resulting gels have been characterized with several techniques: measurement of the melting points (T_{gel}), transparency, gelation time, and viscoelastic properties, together with ECD analysis. Among them, Fmoc-L-Tyr-D-Oxd-OH **1** is an excellent gelator that leads to the preparation of strong, transparent, and viscoelastic gels, by pH variation. UV−visible analyses have demonstrated that the gels obtained with the LMWG **1** possess high transparency, with a transmittance up to 25.6% at a wavelength of 600 nm. Results of the amplitude sweep experiments showed that the elastic response component (G') was approximately an order of magnitude larger than the viscous component, indicating an elastic rather than viscous attitude of the gels, confirmed by the frequency independence of G' and G'' values, in the range from 0.1 to 100 rad·s^{-1}. The thermal behavior of gel obtained from Fmoc-L-Tyr-D-Oxd-OH **1** was characterized performing an "ad hoc" rheological temperature sweep experiment, that indicated that G' remained almost constant from 23 °C up to about 65 °C while G'' increased in the same temperature range. At higher temperatures, both G' and G'' values started to slightly decrease without displaying a crossover point.

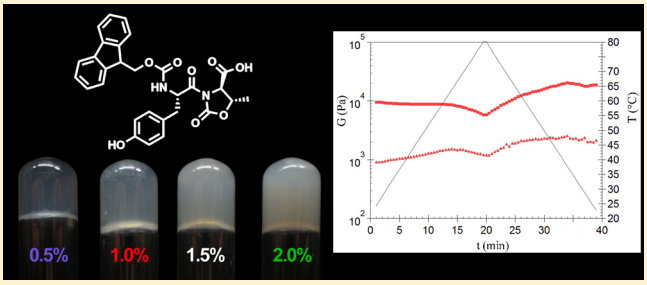

INTRODUCTION

Hydrogels are solidlike materials composed mainly by water,[1−5] as they are formed by a water phase immobilized by a scaffold that results in a gel. Their applications range from the preparation of new materials,[6,7] drug delivery,[8,9] biomineralization,[10,11] growth of cultured cells, mimicking the extracellular matrix,[12−15] and so forth. Polymeric scaffolds are often used, both from natural source (like alginate or pectin) or from synthesis (like cross-linked poly(ethylene oxide) or poly(acrylic acid)), yielding a nonsoluble matrix.[16,17] Hydrogels that are made of covalently cross-linked polymers might have drawbacks: for instance, if cells have to be encapsulated in the gels, the cross-linking process may damage them.[18,19] Moreover, the use of polymeric materials does not permit a precise control of chain length, sequence and three-dimensional (3D) structure. In contrast, self-assembly of molecules into physical hydrogels has the potential to produce precisely defined, hierarchical 3D structures.[20−23]

Low molecular weight gelators (LMWGs) are small molecules able to gelate water and/or organic solvents[24−30] by the formation of reversible supramolecular architectures. They get organized into a 3D structure by supramolecular interactions such as $\pi-\pi$ stacking, hydrophobic and hydrogen bond noncovalent interactions, that favor the formation of layers that in turn get organized into fibers able to trap liquids. A good gelator should immobilize water in a practical and reproducible way, yielding a strong, transparent and flexible gel. Several examples of hydrogels prepared with LMWGs have been recently reported in the literature, but they often suffer of a poor sample homogeneity.[31] Recently, the gelation behavior of Fmoc-protected dipeptides has been studied and reported.[32−34] The hydrogelation process needs to be started by a physical or chemical stimuli, such as an enzymatic,[35] solvent,[36] temperature,[37] or pH[32] trigger.

We have recently reported the preparation of a small library of Fmoc-protected peptidomimetics, containing the L-Phe-D-Oxd unit (or the isosteric L-Phe-D-pGlu unit),[38] [D-Oxd = (4*R*,5*S*)-4-carboxy-5-methyl-oxazoldin-2-one; D-pGlu = D-pyroglutamic acid] that is a privileged scaffold for the preparation of supramolecular materials.[39−43] These moieties have been extensively used by our research group, as we have demonstrated that both pGlu and Oxd, mainly in their D configuration, are able to drive the secondary structure of a peptide chain.[44−47] Both these amino acids are proline analogous, and the presence of the carbonyl moiety inside the pentacyclic ring makes the structure more rigid, placing itself in the *trans* configuration to the carboxyl group. This effect introduces a local constrain that in turn locks the conformation of the peptide chain.

The mechanism through which LMWGs operate depends on a hierarchical self-assembly process which occurs through the following sequence of steps: (i) multiple noncovalent

Received: April 30, 2015
Revised: October 21, 2015
Published: October 22, 2015

DOI: 10.1021/acs.langmuir.5b02780
Langmuir 2015, 31, 12240−12250

interactions between molecular-scale building blocks allow them to self-assemble into supramolecular polymers referred to as fibrils; (ii) the fibrils often then assemble into nanoscale bundles, referred to as fibers; (iii) the fibers tangle and interact with one another to form a self-supporting, sample-spanning "solidlike" network, which underpins the macroscopic gel.

As these compounds have quite different skeletons suggesting that backbone conformation by itself is not enough to justify gelation properties, a rationale to explain the different behavior of these molecules as gelators takes into consideration their hydrophobicity expressed in log *P* (octanol/water partition coefficient),[48] that is calculated as a sum of fragment-based contributions and correction factors. This method is very robust and is able to process practically all organic, and most organometallic molecules.

The best results have been obtained with Fmoc-L-Phe-D-pGlu-OH (log *P* = 3.738), while, much to our surprise, Fmoc-L-Phe-D-Oxd-OH (log *P* = 4.089) proved to be a poor hydrogelator. We could demonstrate that an intermediate value of log *P* (about 3.5−3.8) is a good starting point for the design of new LMWG, as a reduced hydrophilicity reduces its solubility in aqueous solvents and favors gel formation. Unfortunately, none of these compounds displayed an ability to gelate pure water.

Here we want to report some new LMWGs able to gelate water, producing strong, transparent and flexible hydrogels. For this purpose, phenylalanine has been replaced with the aromatic amino acids tryptophan and tyrosine, keeping in mind that a good starting point for the preparation of a good LMWG is that it should have a log *P* value not far from 3.5 to 3.8. To check this assumption, the viscoelastic behavior of these materials has been studied by rheology.

Thus, the purpose of this paper is to study the relationship between small modifications of a well-studied system and the different properties of the produced materials. The aim of this study is thus not only to obtain gel with improved properties, but also to obtain information on the mechanisms behind the gelation processes.

EXPERIMENTAL SECTION

Materials. All chemicals and solvents were purchased by Sigma-Aldrich, VWR, or Iris Biotech and used as received. Acetonitrile was distilled under inert atmosphere before use. Milli-Q water (Millipore, resistivity = 18.2 mΩ·cm) was used throughout.

General Method for the Synthesis of Gelators 1−4. A solution of D-Oxd-OBn or D-pGlu-OBn (1 equiv) in dry acetonitrile was added to a stirred solution of Fmoc-Tyr(*O*-*tert*-Bu)-OH or Fmoc-Trp-OH (1 equiv) and HATU or HBTU (1.1 equiv) at room temperature (RT). After 5 min, a solution of *N*,*N*-diisopropylethylamine or DBU (2.5 equiv) in dry acetonitrile was added to the mixture under inert atmosphere. The solution was stirred for 2 h, then acetonitrile was removed under reduced pressure and replaced with dichloromethane. The mixture was washed with brine, 1 N aqueous HCl, and saturated aqueous $NaHCO_3$, dried over sodium sulfate, and concentrated in vacuo. The coupling product was obtained pure after silica gel chromatography. The *t*-butyl group was removed by reaction of Fmoc-L-Tyr(*O*-*tert*-Bu)-D-Oxd-OBn or Fmoc-L-Tyr(*O*-*tert*-Bu)-D-pGlu-OBn (1 equiv) with trifluoroacetic acid (18 equiv) at RT in dry dichloromethane. The solution was stirred for 4 h under inert atmosphere, and then the mixture was washed with water (3 × 5 mL), dried over sodium sulfate, and concentrated in vacuo. The benzyl esters of all the compounds were transformed into the corresponding carboxylic acids by reaction with Pd/C (10% w/w) under hydrogen atmosphere in methanol at RT for 4 h. The product was obtained pure after filtration through Celite filter and concentrated in vacuo. Detailed synthetic procedure and full characterization data for the intermediate and the final compounds can be found in the Supporting Information (SI).

Log *P* Calculation. All the log *P* values were calculated online with the program http://www.molinspiration.com.

pK_a Determination. A Hamilton Electrochemical Sensor BIOTRODE (pH: 2−11, 0−80 °C) was employed for all measurements. The pK_a values of gelators **1**−**4** (1% w/v) were determined by titration of a basic solution (pH ≈ 11) of the gelator with aliquots of 0.1 M HCl, while stirring the solution to avoid the gel formation. The pK_a values of free D-pGlu and D-Oxd (0.15 M) were evaluated by titration via addition of aliquots of 0.5 M NaOH.

Conditions for the Gel Formation. A portion of compounds **1**−**4** (5−20 mg, depending on the final concentration, ranging from 0.5% to 2% w/w) was placed in a test tube (diameter: 8 mm) and then Milli-Q water (≈0.95 mL) and aqueous NaOH 0.5 N (1.3 equiv for **1** and **2**, 1.0 equiv for **3** and **4**) were added, and the mixture was stirred and sonicated in turn for about 30 min, until sample dissolution. Then glucono-*δ*-lactone (GdL: 1.4 equiv for **1** and **2**, 1.1 equiv for **3** and **4**) was added in one portion to the mixture. After a rapid mixing to allow the GdL complete dissolution, the sample was allowed to stand quiescently until gel formation, that occurs over a number of hours, reaching slowly pH ≈ 5. This method may be applied also to prepare gels in Petri plates, as the gelation procedure is slow enough to transfer the mixture anywhere before solidification.

Conditions for T_{gel} Determination. T_{gel} was determined by heating some test tubes (diameter: 8 mm) containing the gel and a glass ball (diameter: 5 mm; weight: 165 mg) on the top of it. When the gel is formed, the ball is suspended atop. The T_{gel} is a range of temperatures in which the first point indicates when the ball start to penetrate inside the gel, while the second point indicates when the ball touch the bottom of the test tube. Some hydrogel samples melt, producing a clear solution, while in other cases the gelator shrinks and water is ejected, as syneresis occurs.

UV−Vis. A Varian Cary50 UV/vis spectrometer was used. Polystyrene disposable cuvettes (10 mm) were used for all measurements. A reference cuvette was filled with Milli-Q water to autozero the machine. The percent transmission was recorded at a wavelength of 600 nm.

ECD. The CD spectra were recorded on a JASCO spectropolarimeter, model J-815SE, on 0.5% w/w concentration in water in a 0.01 mm quartz cuvette.

Rheology. Rheology experiments were carried out on an Anton Paar rheometer MCR 102 using a parallel plate configuration (25 mm diameter). Experiments were performed at constant temperature of 23 °C controlled via the integrated Peltier system and a Julabo AWC100 cooling system. To keep the sample hydrated, a solvent trap was used (H-PTD200). All the analyses (frequency, amplitude, and temperature sweep analyses) were performed with fixed gap value of 0.5 mm on gel samples prepared directly on the upper plate of the rheometer once the gelation reaction was completed. The samples were prepared the day before the analysis and left overnight to complete the gelation process (around 20 h). Oscillatory amplitude sweep experiments (γ: 0.01−100%) were carried out in order to determine the linear viscoelastic (LVE) range at fixed frequency of 1 rad·s^{-1}. Once the LVE of each gel was established, frequency sweep tests were performed (ω: 0.1−100 rad·s^{-1}) at constant strain within the LVE region of each sample. Time-sweep oscillatory tests were carried out at fixed frequency (1 rad·s^{-1}) and strain amplitude (within the LVE region). In this case, the gelator solution (≈0.5 mL, fresh prepared) was placed in between the two parallel plates and the dynamic moduli were monitored (1 measurement point every 60 s) until a plateau was reached, the plateau was considered reached when the difference between five consecutive acquired G' values was within 0.3%. Temperature sweep experiments were carried out at fixed frequency (1 rad·s^{-1}) and strain amplitude (within the LVE region) by applying to the gels heating and cooling ramps of 3 °C/min from 23 to 80 °C and collecting storage and loss moduli values at fixed measurement point duration.

DOI: 10.1021/acs.langmuir.5b02780
Langmuir 2015, 31, 12240−12250

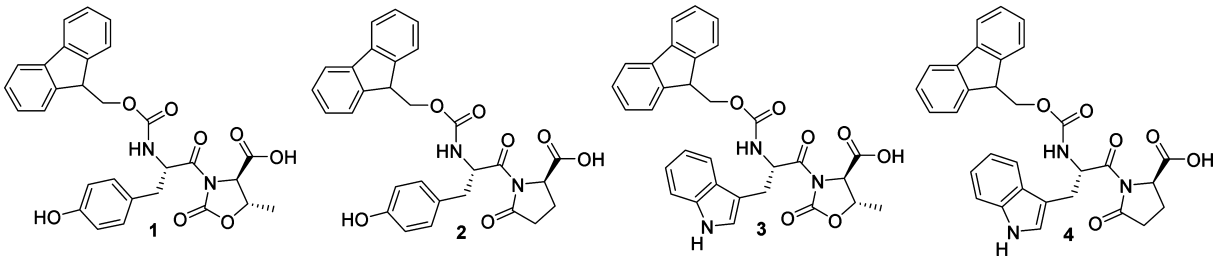

Figure 1. Chemical structures of the compounds described in this work.

SEM Analysis. Scanning electron micrographs of gold-sputtered samples were recorded using a Hitachi 6400 field emission gun scanning electron microscope. The sample was freeze-dried using a BENCHTOP freeze-dry system LABCONCO 7740030 with the following procedure: 0.5 mL of a water mixture containing Fmoc-L-Tyr-D-Oxd-OH **1** in 2% concentration and GdL was poured into an Eppendorf test tube at room temperature. After 24 h, the sample was deeped in liquid nitrogen for 10 min, then it was freeze-dried for 24 h in vacuo (0.2 mbar) at −50 °C. We chose the freeze-drying method to prepare the xerogel sample, because the slow evaporation of the sample causes the collapse of the gelator network, as can be gathered by the SEM images of the xerogel obtained by slow evaporation of the sample (Figure S1).

RESULTS AND DISCUSSION

Synthesis and Characterization of the Gelators 1−4. We have prepared four new LMWGs whose structures are reported in Figure 1. They have been prepared by standard coupling reactions in solution, then the benzyl protective groups have been removed by hydrogenolysis. Compounds **1** and **2** required also the removal of the tyrosine-Boc protecting group by reaction with trifluoroacetic acid in dichloromethane. The simplicity in the preparation of these compounds is therefore an important point in favor of these new kind of gelators.

We previously demonstrated that for this class of peptidomimetics, good LMWGs have a log *P* ranging between 3.5 and 3.8. To check if these peptidomimetics are good candidates to promote hydrogelation, we calculated their log *P* values and we measured their apparent pK_a values (Table 1) to try to rationalize this outcome. Moreover we have measured the pK_a values of unprotected D-Oxd and D-pGlu.

Table 1. Calculated Log *P* Values and Measured pK_a Values of Compounds 1−4 (1% w/w)

molecule	pK_a	log *P*
Fmoc-L-Tyr-D-Oxd-OH **1**	5.4	3.61
Fmoc-L-Tyr-D-pGlu-OH **2**	4.9	3.26
Fmoc-L-Trp-D-Oxd-OH **3**	6.9	4.24
Fmoc-L-Trp-D-pGlu-OH **4**	6.0	3.89

At a first glance, the best LMWG appears to be Fmoc-L-Tyr-D-Oxd−OH **1**, as its log *P* perfectly fits within the 3.5−3.8 range, while **2**−**4** have slightly smaller or slightly bigger log *P* values. We measured also their apparent pK_a: in Figure 2a, we report the titration curve of 1% w/w Fmoc-L-Tyr-D-Oxd-OH as an example, but similar results have been obtained with the other gelators and are reported in the SI (Figures S2−S4). The pK_a values appear to be higher than what expected for a C-terminus peptide, if compared to the pK_a values of free D-Oxd and D-pGlu (pK_a = 2.2 and 2.9, respectively; see Figures S5 and S6), as it has been already observed for other small peptides.[48−50] During the back-titration, we could notice that the molecules tend to precipitate, so the pH of the solution is no more HA concentration dependent since, after reaching the gelator maximum concentration in solution given by its solubility, it remains constant for all the titration, hence reaching the same concentration of [A^-] and [HA] at higher pH values.

As the pK_a shift is probably due to the high hydrophobicity and hence poor solubility of our gelators, this effect can explain the perfect correlation that we obtained between pK_a and log *P* (Figure 2b): higher hydrophobicity means both lower water solubility and higher pK_a.[51]

To further confirm this outcome, we have measured the pK_a values of Fmoc-L-Tyr-D-Oxd-OH **1** in three different concentrations (Table 2; Figures 2a, S7, and S8). We can observe that, on lowering the gelator concentration, the pK_a decreases. Ideally, if we could carry out the pK_a measure at a gelator concentration under the limit of its solubility, we will probably obtain the exact pK_a of our gelators.

Tang et al.[50] also recorded the same results for Fmoc-FF, with a pK_a higher than expected due to its very low solubility. They also found a correlation between pK_a and calculated log *P*, showing an apparent linear relationship, which is similar to what we observed for our gelators (Figure 2b).

Hydrogel Formation. After these preliminary analyses of the properties of the gelators **1**−**4**, their tendency to gelate water has been tested employing the general method adopted in our previous works:[52,53] the samples together with the liquid were placed in a small test tube. Sonication (15 min, 305 W) was used to speed up the dissolution, by breaking intermolecular interactions, then the tubes were left stand still overnight.

Unfortunately, we could never obtain a gel, and thus, we decided to apply a modified method recently described by Adams et al., where the gelators are dissolved in a basic aqueous solution, then glucono-*δ*-lactone (GdL) is added to slowly decrease the solution pH.[54] In fact, all compounds **1**−**4** are totally soluble at pH ≈ 10, while they are totally insoluble at pH ≈ 3, as reported above. If the pH slowly decreases, the pK_a value is reached and the molecules get organized into fibers that in turn trap the water molecules, yielding a hydrogel.[55] To check the gelation efficiency of our molecules, we have submitted to this test also the well described Fmoc-FF as a comparison.

We also tested the gelation behavior of **1**−**4** by decreasing the solution pH value with HCl 1 M instead of GdL. Under these conditions, the gelation process occurs instantaneously, producing a nonhomogeneous gel, with white particulate suspended in the gel. This outcome is not surprising, because we noticed that, on gelator titration with HCl (see above), the pH rapidly decreases from pH ≈ 10 and the stirred solution

DOI: 10.1021/acs.langmuir.5b02780
Langmuir 2015, 31, 12240−12250

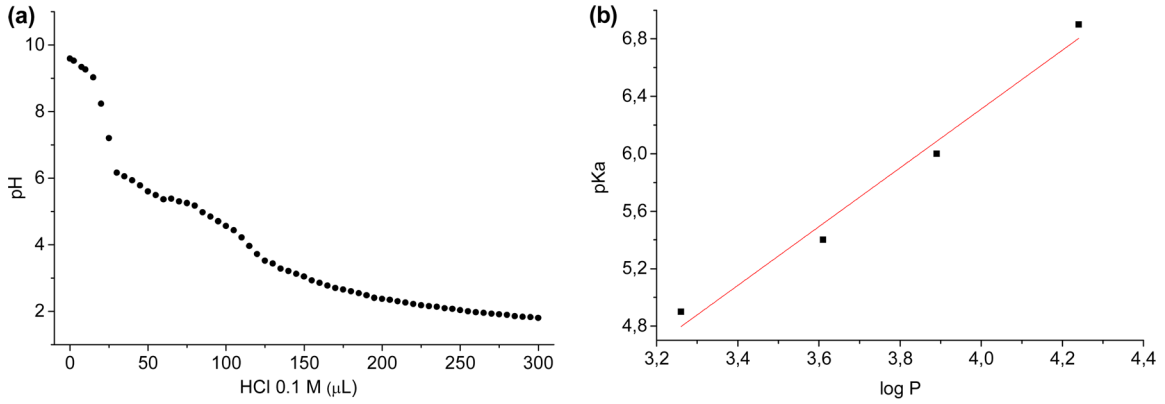

Figure 2. (a) Titration curve (μL of 0.1 M HCl added versus pH) of Fmoc-L-Tyr-D-Oxd-OH **1** (1.0% w/w). (b) Correlation between calculated log *P* and experimental apparent pK_a for compounds **1**–**4**.

Table 2. Measured pK_a Values of Fmoc-L-Tyr-D-Oxd-OH 1 in Three Different Concentrations

concn of **1** (% w/w)	pK_a
0.5	4.6
1.0	5.4
2.0	5.6

becomes progressively cloudy until pH ≈ 6. On further addition of HCl, the solution becomes more viscous and a white precipitate or a hydrogel forms, depending on the pH variation rate. The GdL pH variation method, thanks to the slow process of gelation rate-limited by the hydrolysis of GdL, allows the gelator to self-assembly, yielding homogeneous hydrogels. The final pH of the hydrogels is about 4.5, which is lower than the values of the measured pK_a of our gelators (Table 1).

The gelation behavior of compounds **1**–**4** and of Fmoc-FF has been tested in a concentration ranging between 0.5% and 2.0% w/w. The results are shown in Table 3, together with the gels melting points (T_{gel}).

By a careful analysis of T_{gel}, we could observe different behaviors among our samples: hydrogels obtained with Fmoc-L-Tyr-D-Oxd-OH **1** melt and are totally thermoreversible. In contrast, hydrogels obtained with **2**–**4** are not thermoreversible. In some cases, the gelator melts, then precipitate on cooling, while with in other cases a solution is never obtained, as the gelator shrinks, water is ejected and syneresis occurs. Fmoc-FF leads to the formation of opaque hydrogels that are thermoreversible in concentration ≥1% (w/w) (see the SI for detailed pictures of the hydrogels before and after melting).

An interesting correlation may be found between the calculated log *P* of the gelators and the hydrogel behavior. Fmoc-L-Tyr-D-Oxd-OH **1** has a log *P* value (3.61) that nicely falls between 3.5 and 3.8 and forms thermoreversible hydrogels, while Fmoc-L-Tyr-D-pGlu-OH **2** has a lower log *P* value (3.26) and its hydrogels are not thermoreversible, with the formation of a precipitate on cooling. Finally, the more hydrophobic **3** (log *P* = 4.24) and **4** (log *P* = 3.89) get organized in stable networks that do not break on melting, the hydrogels are not thermoreversible and syneresis occurs. Thermoreversibility is an interesting property which could be useful for several biomedical applications.[56−58]

Thus, Fmoc-L-Tyr-D-Oxd-OH **1** is the only gelator which produces a thermoreversible gel at any concentration. These data suggest that this behavior could be related to the strong interaction of L-Tyr and D-Oxd moieties with water which, also after the breakage of the intramolecular network favored by raising the temperature, this system is able to self-assemble again, confirming that the polarity of the amino acids included inside the peptide chain respect to phenylalanine can influence the final properties of the gels formed. The SEM analysis of the xerogel obtained drying a sample of Fmoc-L-Tyr-D-Oxd-OH **1** hydrogel (Figure 3) is in agreement with these findings, as it shows the formation of locally oriented long strips that cross on the large scale, thus forming a network.

Hydrogel Characterization. The most common diagnostic test of gelation is tube inversion.[59,60] In this test, a sample tube containing the hydrogel is turned upside down to ascertain if the sample would flow under its own weight. A gel is assumed to be a sample that had a yield stress that prevented it from flowing down the tube, while a sol is taken to be a sample that

Table 3. Gelation Properties of Compounds 1−4 in Water as a Function of an Increasing Amount of Gelator (Expressed in % w/w)[a]

	T_{gel}, °C			
compd	0.5% w/w	1.0% w/w	1.5% w/w	2.0% w/w
Fmoc-L-Tyr-D-Oxd-OH **1**	G[be] (55−85)	G[ce] (58−100)	G[ce] (59−100)	G[ce] (66−100)
Fmoc-L-Tyr-D-pGlu-OH **2**	G[cf] (47−70)	G[df] (53−72)	G[df] (57−75)	G[df] (62−82)
Fmoc-L-Trp-D-Oxd-OH **3**	G[bg] (44−100)	G[cg] (55−100)	G[dg] (59−100)	G[dg] (62−100)
Fmoc-L-Trp-D-pGlu-OH **4**	PG	G[dg] (43−100)	G[dg] (52−100)	G[dg] (78−100)
Fmoc-FF	G[dg] (38−100)	G[de] (48−100)	G[de] (60−100)	G[de] (62−100)

[a]The gel melting points (T_{gel}) are reported in parentheses. The gelation properties of Fmoc-FF have been tested in the same conditions for comparison. G = gel; PG = partial gel. [b]Transparent gel. [c]Opalescent gel. [d]Opaque gel. [e]Thermoreversible gel. [f]Not thermoreversible gel, the gelator melts then precipitate on cooling. [g]Not thermoreversible gel, syneresis occurs on heating.

DOI: 10.1021/acs.langmuir.5b02780
Langmuir 2015, 31, 12240−12250

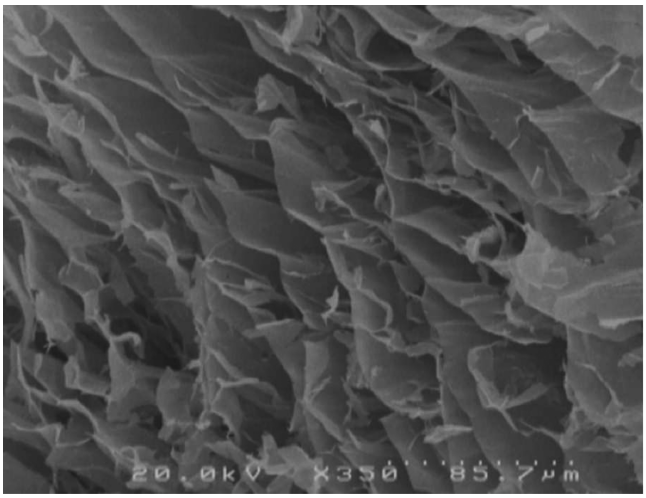

Figure 3. SEM image of a sample of xerogel obtained by freeze-drying a sample of hydrogel prepared with Fmoc-L-Tyr-D-Oxd-OH **1** in 2% concentration.

flowed down the tube. When a partial gel is formed, the compound sticks on the test tube bottom, while little solvent (<20%) flows down.

As depicted in Figure 4, the gels formed by compounds **1** and **3** (Figure 4a and c) at low gelator concentration are rather transparent. This property can be very useful for applications in the field of 3D cell culture, since most of the cells counting methods consist of spectrophotometric analyses, therefore the optical transparency is an indispensable requirement for reliable measurements.[61,62]

To quantify the transparency of our samples, spectroscopic techniques were used to study the influence of the gelator on the gel optical properties.[63,64] UV−visible analysis of the most transparent gel samples have been performed by measuring the % transmittance of the samples recorded at a wavelength of 600 nm, with Milli-Q water used as reference (T = 100%). A gel sample obtained in the same conditions with Fmoc-FF has been analyzed for comparison (Table 4 and Figure S14). Gels

Table 4. % Transmittance of Some Selected Gel Samples Obtained with 1, 3, and Fmoc-FF for Comparison

gelator	% w/w	T (%)
Fmoc-L-Tyr-D-Oxd-OH **1**	0.5	25.6 ± 0.3
Fmoc-L-Tyr-D-Oxd-OH **1**	1.0	6.0 ± 0.1
Fmoc-L-Trp-D-Oxd-OH **3**	0.5	32.1 ± 0.2
Fmoc-L-Trp-D-Oxd-OH **3**	1.0	11.8 ± 0.2
Fmoc-FF	0.5	0.17 ± 0.02

obtained with LMWGs **1** and **3** at 0.5% w/w concentration possess high transparency, as we could measure a transmittance of 25.6% and 32.1% respectively. In contrast, gels obtained with Fmoc-FF showed a low transparency (T = 0.17%).

Another interesting piece of information was obtained by recording the ECD spectra of the hydrogels obtained with a 0.5% w/w concentration of **1**, **3**, and Fmoc-FF (Figure 5). We recorded the first analysis just after adding GdL to the gelator solution (within 10 min) and the second analysis when the gel was formed (after several hours). It should be noted that these measurements were carried out at low concentration (only 0.5% w/w), because at higher concentration strong absorption and light scattering arising from the structures forming on gelation precluded good data collection.[54] Nevertheless, the systems still formed a gel.

In all the spectra, we can notice that CD signals of the molecules before and after gelation are quite similar, thus showing that the molecules get organized in a preferred conformation that is suitable for the formation of fibers that in

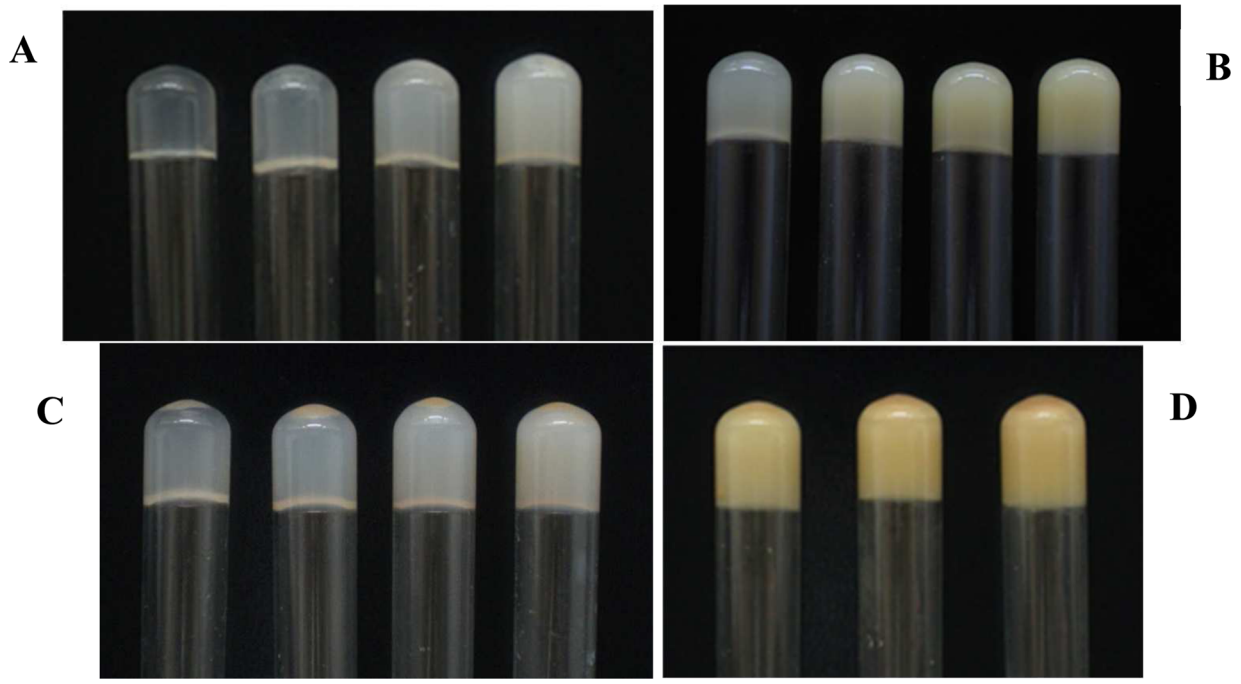

Figure 4. Photographs of hydrogels obtained with compounds **1**−**4** in different concentrations in water (% w/w): (A) Fmoc-L-Tyr-D-Oxd-OH **1**, from left to right: 0.5, 1.0, 1.5, 2.0. (B) Fmoc-L-Tyr-D-pGlu-OH **2**, from left to right: 0.5, 1.0, 1.5, 2.0. (C) Fmoc-L-Trp-D-Oxd-OH **3**, from left to right: 0.5, 1.0, 1.5, 2.0. (D) Fmoc-L-Trp-D-pGlu-OH **4**, from left to right: 1.0, 1.5, 2.0.

DOI: 10.1021/acs.langmuir.5b02780
Langmuir 2015, 31, 12240−12250

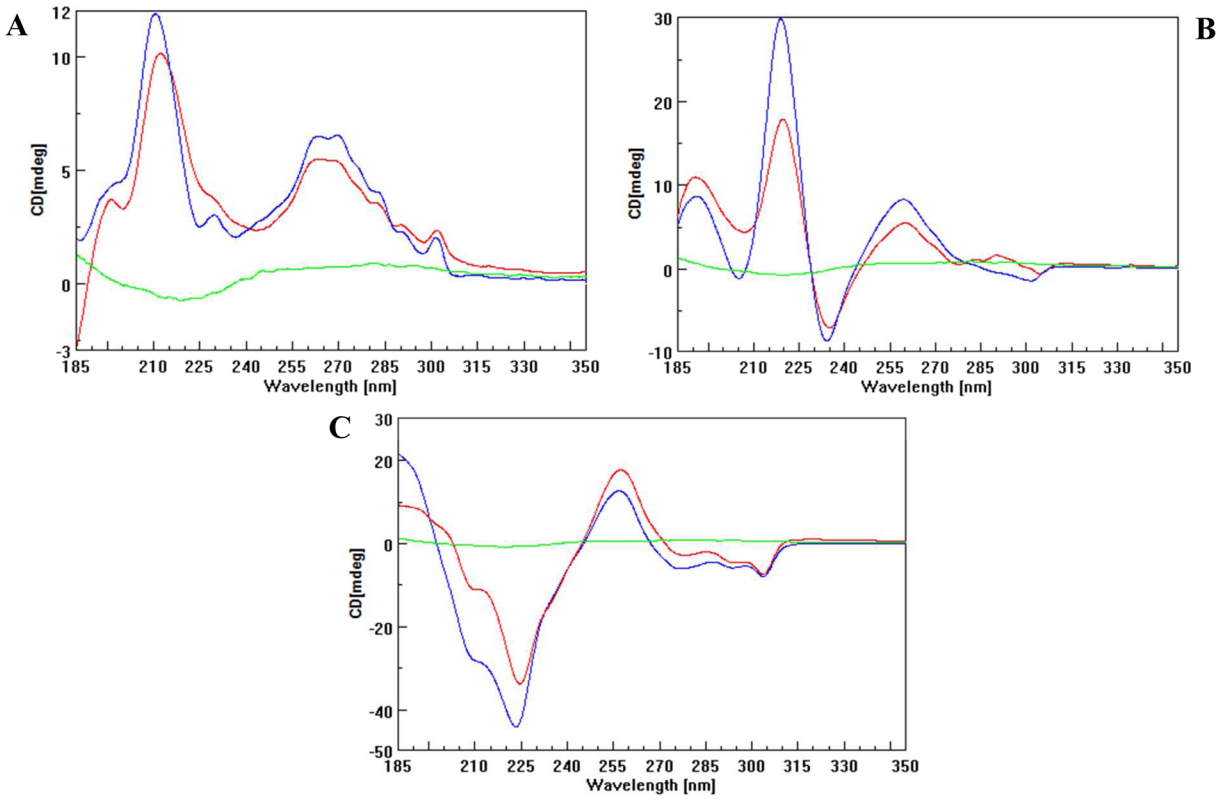

Figure 5. (A) ECD spectra of Fmoc-L-Tyr-D-Oxd-OH **1** in 0.5% w/w concentration in water. (B) ECD spectra of Fmoc-L-Trp-D-Oxd-OH **3** in 0.5% w/w concentration in water. (C) ECD spectra of Fmoc-FF in 0.5% w/w concentration in water. In all the spectra, the green line is the ECD of pure GdL, the blu line is the ECD of gelator and GdL before the gelation occurs, and the red line is the ECD of the hydrogel.

turn end up with the gel formation. GdL by itself does not give significant contribution to CD spectrum; however, one cannot exclude a contribution to CD spectrum when it is trapped in the gel structure. Moreover, no LD effects were observed, by recording the spectra with three orientations (0°, 90° and reverserd). The results are reported in Figures S15–S17.

The CD signals are quite different from one molecule to the other and are all affected by the broad band due to the aromatic chromophore contributions in region about 210 nm.[65]

Our spectrum of Fmoc-FF hydrogel is very similar to the spectrum already reported for this system.[66] The authors attribute the presence of the negative band located at 218 nm to the formation of a β-sheet structure and use as a control sample the ECD spectrum of the nongelling Fmoc-F, that shows two positive peaks at 307 nm and below 214 nm.

If we analyze the spectra of **1** and **3**, we can notice that **3** has a spectrum that resembles the Fmoc-FF spectrum, with a minimum at 235 nm and a maximum at 260 nm, even though **3** contains the D-pGlu moiety. In contrast, the CD spectrum of **1** is all positive and resemble the Fmoc-F spectrum, even though it efficiently forms gels. In any case, due to the aromatic contributions and the presence of D and L configuration residues, one cannot easily associate spectral shapes with secondary structures. Noticeably, the high wavelength band (about 300 nm) due to the Fmoc group shows opposite sign for Fmoc-L-Tyr-D-Oxd-OH **1** and Fmoc-FF, suggesting that this group has a different orientation in the two cases.[67]

Rheological Properties. Rheology studies have been carried out to evaluate the viscoelastic properties of the obtained gels in terms of storage modulus (G'), crossover point (defined as the strain value, in the amplitude sweep curves, at which the G' and G'' curves intersected), and gelation kinetics. It is well-known that these types of experiments are notoriously difficult to perform reproducibly and that the mechanical properties of the gels may vary with the protocol of gel formation[31] and by inherent variability in the preparation procedure of the single specimens within the same protocol. The strength of each gel was evaluated by taking into account the G' values obtained at gelator concentration at 2% and 1% w/w (Table 5, reported values refer to a representative specimen).

Table 5. Storage Modulus (G'), Linear Viscoelastic Region (LVE) and Crossover Point of Compounds 1–4 at 2% w/w and 1% w/w[a]

compd	concn (% w/w)	G' (Pa)[b]	LVE (γ %)[b]	crossover point (γ %)[b]
Fmoc-L-Tyr-D-Oxd-OH **1**	2	52 600	1	11
	1	6000	2	15
Fmoc-L-Tyr-D-pGlu-OH **2**	2	30 000	1	5
	1	12 000	3	9
Fmoc-L-Trp-D-Oxd-OH **3**	2	31 600	1	6
	1	7000	3	9
Fmoc-L-Trp-D-pGlu-OH **4**	2	36 000	1	5
	1	3000	2	33
Fmoc-FF	2	100 000	0.18	4
	1	10 000	1	9

[a]Results of Fmoc-FF at 2% w/w and 1% w/w are also shown. [b]The analyses were performed on the gels about 20 h after the gelation begun.

DOI: 10.1021/acs.langmuir.5b02780
Langmuir 2015, 31, 12240–12250

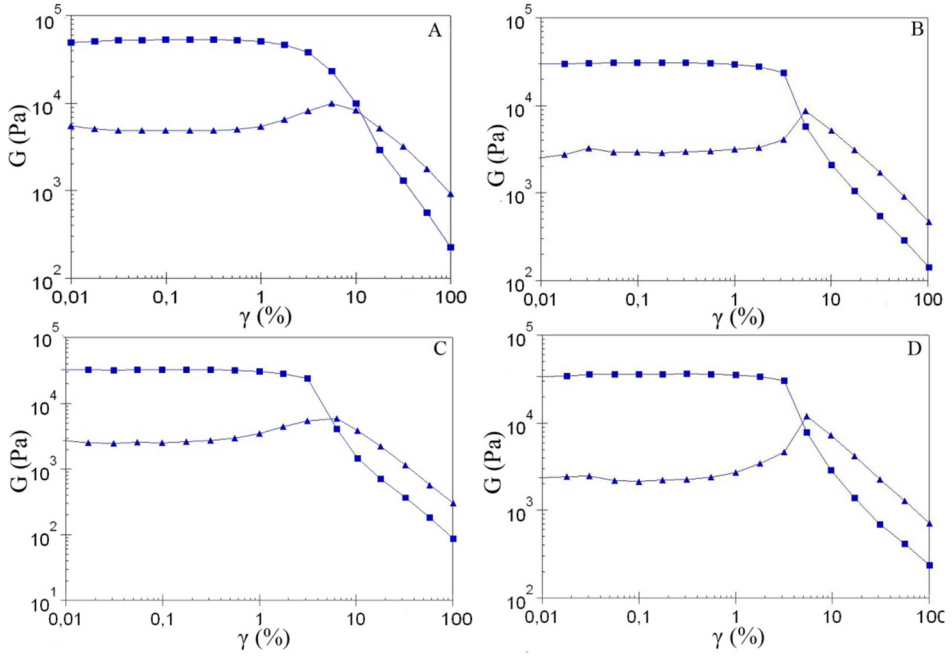

Figure 6. Strain dependence of storage modulus (square) and loss modulus (triangle) at 2% w/w gelator concentration of (A) Fmoc-L-Tyr-D-Oxd-OH **1**, (B) Fmoc-L-Tyr-D-pGlu-OH **2**, (C) Fmoc-L-Trp-D-Oxd-OH **3**, and (D) Fmoc-L-Trp-D-pGlu-OH **4**. The analyses were performed on the gels about 20 h after the gelation begun.

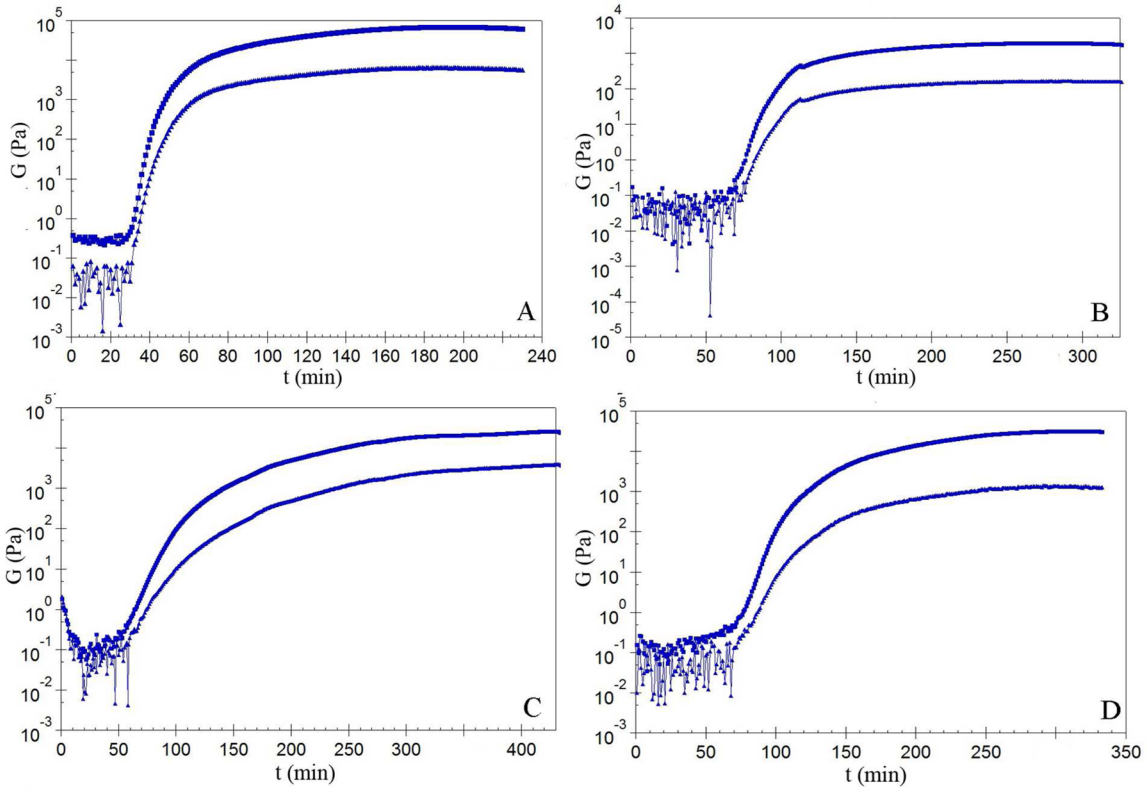

Figure 7. Time dependence of storage modulus and loss modulus for gels obtained starting from (A) Fmoc-L-Tyr-D-Oxd-OH **1**, (B) Fmoc-L-Tyr-D-pGlu-OH **2**, (C) Fmoc-L-Trp-D-Oxd-OH **3**, and (D) Fmoc-L-Trp-D-pGlu-OH **4** at fixed gelator concentration of 2% w/w. The analyses were performed on the gels about 20 h after the gelation begun.

For each gel, at fixed gelator concentration of 2% w/w, a constant G' value at strain within 1% (linear viscoelastic behavior) was found. Results of the amplitude sweep experiments for compounds **1**−**4** at 2% w/w concentration (Figure 6) showed that the elastic response component (G') was approximately an order of magnitude larger than the viscous component (G'', loss modulus), indicating a "solidlike" attitude of the gels. Measurements of the moduli as a function

DOI: 10.1021/acs.langmuir.5b02780
Langmuir 2015, 31, 12240−12250

of frequency (Figure S18) pointed out that both G' and G'' were almost independent from the frequency in the range from 0.1 to 100 rad·s^{-1} (with G' always greater than G'') confirming the "solidlike" rheological behavior for the analyzed gels. To check the efficiency of our molecules, we evaluated also the strength of the gel obtained from Fmoc-FF as a comparison (Figure S19). A similar behavior was also found for the gels obtained from compounds **1**−**4** and Fmoc-FF at 1% w/w (Table 5 and Figure S20).

If we compare the gels obtained from our compounds **1**−**4** at fixed gelator concentration of 2% w/w, we can gather that those obtained from compound **1** show the highest G' value indicating that it is the stiffest gel even though weaker than what obtained from Fmoc-FF at the same concentration. Compounds **2** and **3** at 2% w/w produce gels characterized by similar G' values, lower than that of compound **1**, whereas compound **4** leads to gels showing an intermediate G' value.

It is worth mentioning that the crossover point of compound **1** is reached at higher strain (11%) than the other gels, all ranging between 4 and 6%. Since this parameter represents the deformation value at which the solid gel-like character of the material ($G' > G''$) changes to the "liquid-state" ($G'' > G'$), comparison of the crossover point values suggests that compound **1**, besides being the strongest gel among the synthesized ones (higher G'), is characterized by a greater resistance to deformation. Interestingly, Fmoc-FF shows the lowest strain value at the crossover point (4%) (Figure S19), indicating that all the gels obtained from gelators **1**−**4** maintained the elastic, "solidlike" behavior also at deformations at which the Fmoc-FF gel lose its stability, assuming a viscous, "liquidlike" character.

The kinetic behavior of the gels obtained from the compounds **1**−**4** at 2% w/w concentration was monitored through time sweep experiments (Figure 7). It is worth noticing that the slight decrease of G' at the end of the gelation process, observed in the obtained curves, might be related to syneresis due to long-standing of the material under stress conditions, whereas the sharp gradient and the little dip in G' and G'' in data set B was attributed to slippage. The obtained curves show a similar kinetics behavior and it appears that the hydrogel formation is a one-step process. Both storage and loss modulus increase reaching a constant G' and G'' values at different times, quoted in Table 6. Fmoc-L-Tyr-D-Oxd-OH **1** possess the lowest gelation time suggesting that the fast hydrogel formation is related to the highest storage modulus value (Table 5). Interestingly gels obtained from LMWG **1** show G' values of 1 order of magnitude higher compared to G'' values even from the beginning of the gelification process. Furthermore, both moduli are higher than the other gelators at the beginning of the gelation process.

Table 6. Gelation Time of Compound 1 at 2% w/w and 1% w/w and of Compounds 2−4 at 2% w/w

compd	concn (% w/w)	gelation time (min)[a]
Fmoc-L-Tyr-D-Oxd-OH **1**	2	196
	1	325
Fmoc-L-Tyr-D-pGlu-OH **2**	2	300
Fmoc-L-Trp-D-Oxd-OH **3**	2	430
Fmoc-L-Trp-D-pGlu-OH **4**	2	321

[a]Gelation time values are quoted as the time needed to reach a constant G' value (the plateau was considered reached when the difference between five consecutive acquired G' values was within 0.3%).

As Fmoc-L-Tyr-D-Oxd-OH **1** is the most promising gelator among the synthesized ones, the effect of the concentration on its gel viscoelastic properties and the kinetics of the gel formation was studied by means of amplitude sweep (Figure 8A) and time sweep (Figure 8B) experiments, respectively. The comparison between the amplitude sweep curves in Figure 8A pointed out that the decrease of the gelator concentration from 2% to 1% w/w causes both a shift in the LVE range limit toward higher values (from 1% to 2%) and a decrease of the G' values (Table 5). In addition, parallel to the LVE trend, the crossover point of the gels obtained from LMWG **1** increased with the decrease of concentration from 11% for 2% w/w gel to 15% for 1% w/w gel) (Table 5).

To better understand the influence of the gelator concentration not only on gels properties in terms of stiffness, but also on the gel formation, the gelation process for compound **1** was monitored through time sweep experiments (Figure 8B). Kinetics studies demonstrated that the decrease of the gelator concentration led to the increase of the gelation time (Table 6), that is, the time needed to reach a constant G' values (the plateau value was considered reached when the difference between five consecutive acquired G' values was within 0.3%).

In order to gain further insights on the kind of network formed for gel obtained from LMWG 1, the storage moduli of the obtained gels at different concentration of 2%, 1.5%, and 1% w/w were plotted against gelator concentration (Figure S21). The storage moduli scaled with the gelator concentration with an exponent of 3. This value is slightly higher compared to those typically found for cross-linked network that usually are around 2.5,[63] whereas it is the lowest value reported for colloidal gels. In the latter systems usually storage moduli scale with the gelator concentration with an exponent between 3 and 6.[68−70]

Finally, the thermal behavior of gels obtained starting from LMWGs **1** and **3** and Fmoc-FF at 1% w/w gelator concentration was explored by performing an "ad hoc" rheological temperature sweep experiment (Figure 9).[71]

For the gel obtained from Fmoc-L-Tyr-D-Oxd−OH **1** (Figure 9A), G' remained almost constant from 23 °C up to about 65 °C while G'' increased in the same temperature range. At higher temperatures, both G' and G'' values started to slightly decrease without displaying a crossover point. This behavior might be attributed to a slight loss of network stability, while maintaining the gel-like structure. During the cooling cycle, from 80 to 23 °C, both G' and G'' increased reaching higher values compared to the starting ones, a behavior that can be related to water evaporation from gel network. A similar behavior can be found for the gel obtained from Fmoc-FF (Figure 9C), with G' almost independent from temperature from 23 °C to around 55 °C and G'' values that started to increase in the same temperature range. From 55 to 80 °C and even during cooling down to 23 °C, both G' and G'' increased reaching higher values compared to the starting ones, showing a behavior similar to that of LMWG **1**. In contrast, the curve obtained for the Fmoc-L-Trp-D-Oxd-OH **3** gel reported in Figure 9B shows an almost independent temperature behavior of both G' and G'' values from 23 °C to around 70 °C, followed by a decrease of G' and G'' from 70 to 23 °C. This outcome can be related to the loss of stability of the molecular network that is not recovered during the cooling cycle, typical of a nonthermoreversible gel.

DOI: 10.1021/acs.langmuir.5b02780
Langmuir 2015, 31, 12240−12250

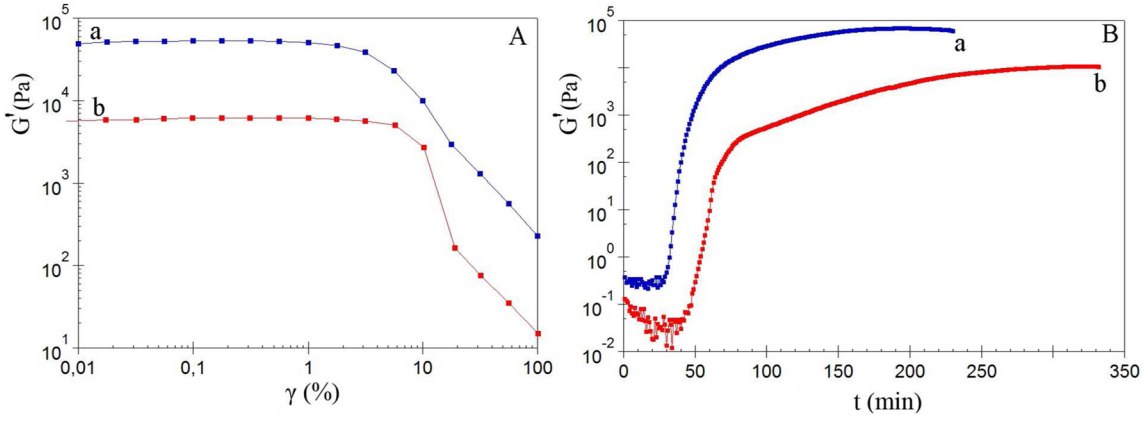

Figure 8. Effect of the concentration on (A) storage modulus and (B) gel formation kinetics for Fmoc-L-Tyr-D-Oxd-OH **1** at (a) 2% w/w (b) 1% w/w. The analyses were performed on the gels about 20 h after the gelation begun.

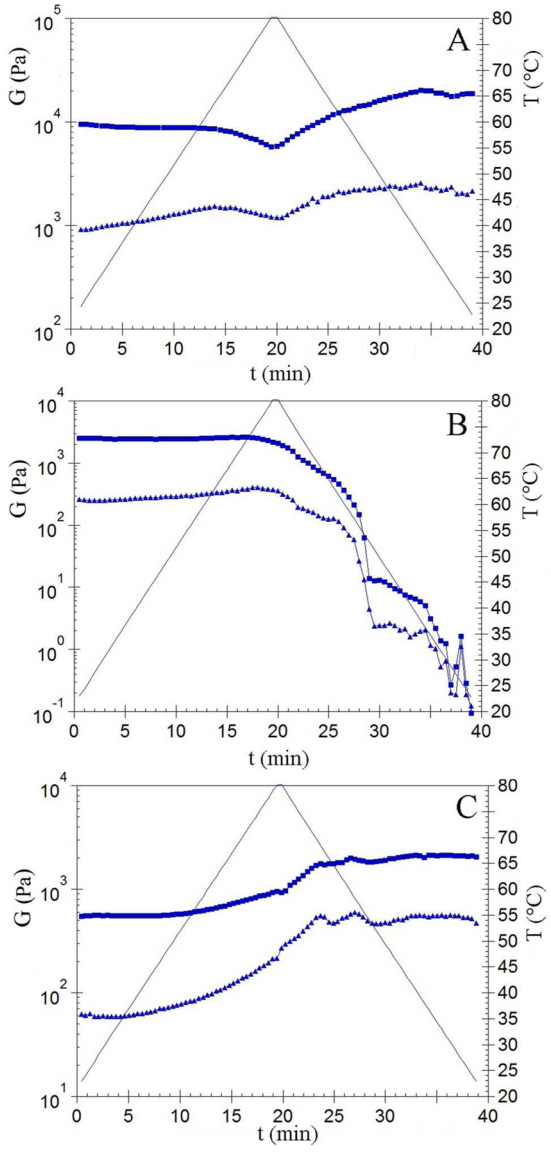

Figure 9. Temperature dependence of G' (squares) and G'' (triangles) for gels obtained from (A) Fmoc-L-Tyr-D-Oxd-OH **1**, (B) Fmoc-L-Trp-D-Oxd-OH **3**, and (C) Fmoc-FF, all at 1% w/w gelator concentration. Continuous line represents the heating and cooling ramp.

Thus, comparing the rheological thermal behavior of the three gelators shown in Figure 9, we can conclude that while gels obtained from Fmoc-L-Tyr-D-Oxd-OH **1** and from Fmoc-FF in 1% w/w concentration create networks able to resist to the applied temperature ramp, the gels obtained from Fmoc-L-Trp-D-Oxd-OH **3** possess a molecular network less stable to temperature.

CONCLUSIONS

We have prepared four new Fmoc-protected peptidomimetics **1**−**4** by standard coupling reaction in solution. The preparation is straightforward so compounds **1**−**4** can be easily obtained in multigram scale. All these compounds are good hydrogelators. The gelation trigger is the pH variation, as glucono-δ-lactone (GdL) was added to a basic aqueous solution of the gelator. The resulting gels have been characterized by using several techniques: measurement of the melting point (T_{gel}), of the transparency, and of the viscoelastic properties, ECD analysis and gelation time. From all these data, we could demonstrate that Fmoc-L-Tyr-D-Oxd-OH **1** is an excellent gelator that leads to the preparation of strong and transparent gels characterize by excellent viscoelastic properties, through a simple and reproducible method. Results of the amplitude sweep experiments for compounds **1**−**4** at 2% w/w concentration (Figure 5) showed that the elastic response component (G') was approximately an order of magnitude larger than the viscous component (G'', loss modulus) in any case, indicating a "solidlike" attitude of the gels. Measurements of the moduli as a function of frequency pointed out that both G' and G'' were almost independent from the frequency in the range from 0.1 to 100 rad·s^{-1} confirming the "solidlike" rheological behavior for the analyzed gels. Finally, the thermal behavior of the most promising gels were characterized by performing an "ad hoc" rheological temperature sweep experiment, that demonstrated that for the gel obtained from Fmoc-L-Tyr-D-Oxd-OH **1** G' remained almost constant from 23 °C up to about 65 °C while G'' increased in the same temperature range. At higher temperatures, both G' and G'' values started to slightly decrease without displaying a crossover point. This result is in agreement with our previous findings, indicating that this is a well-built, thermoreversible gel.

DOI: 10.1021/acs.langmuir.5b02780
Langmuir 2015, 31, 12240−12250

■ ASSOCIATED CONTENT

Supporting Information

The Supporting Information is available free of charge on the ACS Publications website at DOI: 10.1021/acs.langmuir.5b02780.

Synthetic scheme and synthetic details for the preparation of compounds **1**−**4**; characterization of compounds **1**−**4**; SEM image of xerogel from **1**, obtained by slow evaporation of the sample; titration curve of compounds **1**−**4**, H-D-Oxd-OH and H-D-pGlu-OH; photographs of samples of hydrogels from **1**−**4** and Fmoc-FF after melting and after cooling down; picture of the gels obtained in cuvettes for visible analysis; ECD, HT and Abs spectra of **1**, **3**, and Fmoc-FF, recorded with three orientation (0°, 90°, and reversed); frequency dependence of storage modulus and loss modulus for gels obtained starting from compounds **1**−**4** at 2% w/w concentration; strain dependence and frequency dependence of storage modulus and loss modulus for gels obtained starting from compounds **1**−**4** at 1% w/w and Fmoc-FF at 2% and 1% w/w concentration; strain dependence of storage modulus and loss modulus for gels obtained from compound **1** at 1.5% w/w concentration; concentration dependence of storage moduli for gels obtained from compound **1** (PDF)

■ AUTHOR INFORMATION

Corresponding Authors

*E-mail: claudia.tomasini@unibo.it.

*E-mail: marialetizia.focarete@unibo.it.

Notes

The authors declare no competing financial interest.

■ ACKNOWLEDGMENTS

We thank Prof. Giovanna Longhi (Dipartimento di Medicina Molecolare e Traslazionale - Università degli Studi di Brescia) for helpful discussions on the ECD spectra. C.T. thanks "Ministero dell'Istruzione, dell'Università e della Ricerca" (MIUR) (program PRIN 2010NRREPL_009). L.M. thanks "Consorzio Spinner Regione Emilia Romagna" for financial support.

■ REFERENCES

(1) Wade, R. J.; Bassin, E. J.; Gramlich, W. M.; Burdick, J. A. Nanofibrous Hydrogels with Spatially Patterned Biochemical Signals to Control Cell Behavior. *Adv. Mater.* **2015**, *27*, 1356−1362.

(2) Toh, W. S.; Loh, X. J. Advances in hydrogel delivery systems for tissue regeneration. *Mater. Sci. Eng., C* **2014**, *45*, 690−697.

(3) Hoffman, A. S. Hydrogels for biomedical applications. *Adv. Drug Delivery Rev.* **2002**, *54*, 3−12.

(4) Seliktar, D. Designing Cell-Compatible Hydrogels for Biomedical Applications. *Science* **2012**, *336*, 1124−1128.

(5) Appel, E. A.; Del Barrio, J.; Loh, X. J.; Scherman, O. A. Supramolecular polymeric hydrogels. *Chem. Soc. Rev.* **2012**, *41*, 6195−6214.

(6) Praveen, V. K.; Ranjith, C.; Armaroli, N. White-Light-Emitting Supramolecular Gels. *Angew. Chem., Int. Ed.* **2014**, *53*, 365−368.

(7) Xing, P.; Chu, X.; Li, S.; Ma, M.; Hao, A. Hybrid Gels Assembled from Fmoc-Amino Acid and Graphene Oxide with Controllable Properties. *ChemPhysChem* **2014**, *15*, 2377−2385.

(8) Bibian, M.; Mangelschots, J.; Gardiner, J.; Waddington, L.; Diaz Acevedo, M. M.; De Geest, B. G.; Van Mele, B.; Madder, A.; Hoogenboom, R.; Ballet, S. Rational design of a hexapeptide hydrogelator for controlled-release drug delivery. *J. Mater. Chem. B* **2015**, *3*, 759−765.

(9) Skilling, K. J.; Citossi, F.; Bradshaw, T. D.; Ashford, M.; Kellam, B.; Marlow, M. Insights into low molecular mass organic gelators: a focus on drug delivery and tissue engineering applications. *Soft Matter* **2014**, *10*, 237−256.

(10) Hartgerink, J. D.; Beniash, E.; Stupp, S. I. Self-Assembly and Mineralization of Peptide-Amphiphile Nanofibres. *Science* **2001**, *294*, 1684−1688.

(11) Tomasini, C.; Castellucci, N.; Caputo, V. C.; Milli, L.; Battistelli, G.; Fermani, S.; Falini, G. Shaping calcite crystals by customized self-assembling pseudopeptide foldamers. *CrystEngComm* **2015**, *17*, 116−123.

(12) Narmoneva, D. A.; Oni, O.; Sieminski, A. L.; Zhang, S. G.; Gertler, J. P.; Kamm, R. D.; Lee, R. T. Self-assembling short oligopeptides and the promotion of angiogenesis. *Biomaterials* **2005**, *26*, 4837−4846.

(13) Bokhari, M. A.; Akay, G.; Zhang, S. G.; Birch, M. A. The enhancement of osteoblast growth and differentiation in vitro on a peptide hydrogel-polyHIPE polymer hybrid material. *Biomaterials* **2005**, *26*, 5198−5208.

(14) Schneider, J. P.; Pochan, D. J.; Ozbas, B.; Rajagopal, K.; Pakstis, L.; Kretsinger, J. Responsive Hydrogels from the Intramolecular Folding and Self-Assembly of a Designed Peptide. *J. Am. Chem. Soc.* **2002**, *124*, 15030−15037.

(15) Ellis-Behnke, R. G.; Liang, Y. X.; You, S. W.; Tay, D. K. C.; Zhang, S. G.; So, K. F.; Schneider, G. E. Nano neuro knitting: Peptide nanofiber scaffold for brain repair and axon regeneration with functional return of vision. *Proc. Natl. Acad. Sci. U. S. A.* **2006**, *103*, 5054−5059.

(16) Voldřich, Z.; Tomnek, Z.; Vacìk, J.; Kopeček, J. Long-term experience with poly(glycol monomethacrylate) gel in plastic operations of the nose. *J. Biomed. Mater. Res.* **1975**, *9*, 675−685.

(17) Wichterle, O. Reshaping a xerogel by mechanical removal and swelling from a hydrogel contact lens. U.S. Patent 3361858, 1968.

(18) Ifkovits, J. L.; Burdick, J. A. Photopolymerizable and Degradable Biomaterials for Tissue Engineering Applications. *Tissue Eng.* **2007**, *13*, 2369−2385.

(19) Krishna, O. D.; Kiick, K. L. Protein- and peptide-modified synthetic polymeric biomaterials. *Biopolymers* **2010**, *94*, 32−48.

(20) Kopeček, J.; Yang, J. Peptide-directed self-assembly of hydrogels. *Acta Biomater.* **2009**, *5*, 805−816.

(21) Xu, C.; Kopeček, J. Self-Assembling Hydrogels. *Polym. Bull.* **2007**, *58*, 53−63.

(22) Kopeček, J. Smart and genetically engineered biomaterials and drug delivery systems. *Eur. J. Pharm. Sci.* **2003**, *20*, 1−16.

(23) Fleming, S.; Ulijn, R. V. Design of nanostructures based on aromatic peptide amphiphiles. *Chem. Soc. Rev.* **2014**, *43*, 8150−8177.

(24) Adams, D. J. Dipeptide and Tripeptide Conjugates as Low-Molecular-Weight Hydrogelators. *Macromol. Biosci.* **2011**, *11*, 160−173.

(25) Adams, D. J.; Topham, P. D. Peptide conjugate hydrogelators. *Soft Matter* **2010**, *6*, 3707−3721.

(26) Gao, Y.; Zhao, F.; Wang, Q.; Zhang, Y.; Xu, B. Small peptide nanofibers as the matrices of molecular hydrogels for mimicking enzymes and enhancing the activity of enzymes. *Chem. Soc. Rev.* **2010**, *39*, 3425−3433.

(27) Babu, S. S.; Praveen, V. K.; Ajayaghosh, A. Functional π-Gelators and Their Applications. *Chem. Rev.* **2014**, *114*, 1973−2129.

(28) Tomasini, C.; Castellucci, N. Peptides and peptidomimetics that behave as low molecular weight gelators. *Chem. Soc. Rev.* **2013**, *42*, 156−172.

(29) Fichman, G.; Gazit, E. Self-assembly of short peptides to form hydrogels: Design of building block, physical properties and technological. *Acta Biomater.* **2014**, *10*, 1671−1682.

(30) Johnson, E. K.; Adams, D. J.; Cameron, P. J. Peptide based low molecular weight gelators. *J. Mater. Chem.* **2011**, *21*, 2024−2027.

DOI: 10.1021/acs.langmuir.5b02780
Langmuir 2015, 31, 12240−12250

(31) Raeburn, J.; Pont, G.; Chen, L.; Cesbron, Y.; Levy, R.; Adams, D. J. Fmoc-diphenylalanine hydrogels: understanding the variability in reported mechanical properties. *Soft Matter* **2012**, *8*, 1168−1174.
(32) Jayawarna, V.; Ali, M.; Jowitt, T. A.; Miller, A. E.; Saiani, A.; Gough, J. E.; Ulijn, R. V. Nanostructured Hydrogels for Three-Dimensional Cell Culture Through Self-Assembly of Fluorenylmethoxycarbonyl-Dipeptides. *Adv. Mater.* **2006**, *18*, 611−614.
(33) Jayawarna, V.; Richardson, S. M.; Hirst, A. R.; Hodson, N. W.; Saiani, A.; Gough, J. E.; Ulijn, R. V. Introducing chemical functionality in Fmoc-peptide gels for cell culture. *Acta Biomater.* **2009**, *5*, 934−943.
(34) Jayawarna, V.; Smith, A.; Gough, J. E.; Ulijn, R. V. Three-dimensional cell culture of chondrocytes on modified di-phenylalanine. *Biochem. Soc. Trans.* **2007**, *35*, 535−537.
(35) Williams, R. J.; Smith, A. M.; Collins, R.; Hodson, N.; Das, A. K.; Ulijn, R. V. Enzyme-assisted self-assembly under thermodynamic control. *Nat. Nanotechnol.* **2009**, *4*, 19−24.
(36) Orbach, R.; Adler-Abramovich, L.; Zigerson, S.; Mironi-Harpaz, I.; Seliktar, D.; Gazit, E. Self-Assembled Fmoc-Peptides as a Platform for the Formation of Nanostructures and Hydrogels. *Biomacromolecules* **2009**, *10*, 2646−2651.
(37) Vegners, R.; Shestakova, I.; Kalvinsh, I.; Ezzell, R. M.; Janmey, P. A. Use of a gel-formig dipeptide derivative as a carrier for antigen presentation. *J. Pept. Sci.* **1995**, *1*, 371−378.
(38) Milli, L.; Castellucci, N.; Tomasini, C. Turnig Around the L-Phe-D-Oxd Moiety for a Versatile Low-Molecular-Weight Gelator. *Eur. J. Org. Chem.* **2014**, *2014*, 5954−5961.
(39) Tomasini, C.; Angelici, G.; Castellucci, N. Foldamers Based on Oxazolidin-2-ones. *Eur. J. Org. Chem.* **2011**, *2011*, 3648−3669.
(40) Angelici, G.; Falini, G.; Hofmann, H.-J.; Huster, D.; Monari, M.; Tomasini, C. A Fiberlike Peptide Material Stabilized by Single Intermolecular Hydrogen Bonds. *Angew. Chem., Int. Ed.* **2008**, *47*, 8075−8078.
(41) Angelici, G.; Falini, G.; Hofmann, H.-J.; Huster, D.; Monari, M.; Tomasini, C. Nanofibers from Oxazolidin-2-one Containing Hybrid Foldames: What is the Right Molecular Size? *Chem. - Eur. J.* **2009**, *15*, 8037−8048.
(42) Castellucci, N.; Angelici, G.; Falini, G.; Monari, M.; Tomasini, C. L-Phe-D-Oxd: A Privileged Scaffold for the Formation of Supramolecular Materials. *Eur. J. Org. Chem.* **2011**, *2011*, 3082−3088.
(43) Scheidt, H. A.; Sickert, A.; Meier, T.; Castellucci, N.; Tomasini, C.; Huster, D. The interaction of lipid modified pseudopeptides with lipid membranes. *Org. Biomol. Chem.* **2011**, *9*, 6998−7006.
(44) Luppi, G.; Lanci, D.; Trigari, V.; Garavelli, M.; Garelli, A.; Tomasini, C. Development and Conformational Analysis of a Pseudoproline-Containing β-Turn Mimic. *J. Org. Chem.* **2003**, *68*, 1982−1993.
(45) Tomasini, C.; Luppi, G.; Monari, M. Oxazolidin-2-ones-Containing Pseudopeptides that Fold into β-Bend Ribbon Spirals. *J. Am. Chem. Soc.* **2006**, *128*, 2410−2420.
(46) Angelici, G.; Luppi, G.; Kaptein, B.; Broxterman, Q. B.; Hofmann, H.-J.; Tomasini, C. Synthesis and Secondary Structure of Alternate α,β-Hybrid Peptides Containing Oxazolidin-2-one Moieties. *Eur. J. Org. Chem.* **2007**, *2007*, 2713−2721.
(47) Longhi, G.; Abbate, S.; Lebon, F.; Castellucci, N.; Sabatino, P.; Tomasini, C. Conformational Studies of Phe-rich foldamers by VCD spectroscopy and ab-initio calculations. *J. Org. Chem.* **2012**, *77*, 6033−6042.
(48) Adams, D. J.; Mullen, L. M.; Berta, M.; Chen, L.; Frith, W. J. Relationship between molecular structure, gelation behavior and gel properties of Fmoc-dipeptides. *Soft Matter* **2010**, *6*, 1971−1980.
(49) Chen, L.; Morris, K.; Laybourn, A.; Elias, D.; Hicks, M. R.; Rodger, A.; Serpell, L.; Adams, D. J. Self-Assembly Mechanism for a Naphthalene-Dipeptide Leading to Hydrogelation. *Langmuir* **2010**, *26*, 5232−5242.
(50) Tang, C.; Smith, A. M.; Collins, R. F.; Ulijn, R. V.; Saiani, A. Fmoc-Diphenylalanine Self-Assembly Mechanism Induces Apparent pK_a Shifts. *Langmuir* **2009**, *25*, 9447−9453.
(51) Chen, L.; Revel, S.; Morris, K.; Serpell, L. C.; Adams, D. J. Effect of Molecular Structure on the Properties of Naphthalene-Dipeptide Hydrogelators. *Langmuir* **2010**, *26*, 13466−13471.
(52) Castellucci, N.; Falini, G.; Angelici, G.; Tomasini, C. Formation of gels in the presence of metal ions. *Amino Acids* **2011**, *41*, 609−620.
(53) Castellucci, N.; Sartor, G.; Calonghi, N.; Parolin, C.; Falini, G.; Tomasini, C. A peptidic hydrogel that may behave as a "Trojan Horse. *Beilstein J. Org. Chem.* **2013**, *9*, 417−424.
(54) Adams, D. J.; Butler, M. F.; Frith, W. J.; Kirkland, M.; Mullen, L.; Sanderson, P. A new method for maintaining homogeneity during liquid-hydrogel transitions using low molecular weight hydrogelators. *Soft Matter* **2009**, *5*, 1856−1862.
(55) Frisch, H.; Besenius, P. pH-Switchable Self-Assembled Materials. *Macromol. Rapid Commun.* **2015**, *36*, 346−363.
(56) Pratoomsoot, C.; Tanioka, H.; Hori, K.; Kawasaki, S.; Kinoshita, S.; Tighe, P. J.; Dua, H.; Shakesheff, K. M.; Rose, F. R. A. J. A thermoreversible hydrogel as a biosynthetic bandage for corneal wound repair. *Biomaterials* **2008**, *29*, 272−281.
(57) Wang, D.; Cheng, D.; Guan, Y.; Zhang, Y. Thermoreversible Hydrogel for *In Situ* Generation and Release of HepG2 Spheroids. *Biomacromolecules* **2011**, *12*, 578−584.
(58) Tsao, C. T.; Kievit, F. M.; Wang, K.; Erickson, A. E.; Ellenbogen, R. G.; Zhang, M. Chitosan-Based Thermoreversible Hydrogel as an in Vitro Tumor Microenvironment for Testing Breast Cancer Therapies. *Mol. Pharmaceutics* **2014**, *11*, 2134−2142.
(59) Takahashi, K.; Sakai, M.; Kato, T. Melting Temperature of Thermally Reversible Gel. VI. Effect of Branching on the Sol-Gel Transition of Polyethylene Gels. *Polym. J.* **1980**, *12*, 335−341.
(60) Yamanaka, M.; Fujii, H. Chloroalkane Gel Formations by Tris-urea Low Molecular Weight Gelator under Various Conditions. *J. Org. Chem.* **2009**, *74*, 5390−5394.
(61) Wang, H.; Yang, Z.; Adams, D. J. Controlling peptidebased hydrogelation. *Mater. Today* **2012**, *15*, 500−507.
(62) Li, C.; Faulkner-Jones, A.; Dun, A. R.; Jin, J.; Chen, P.; Xing, Y.; Yang, Z.; Li, Z.; Shu, W.; Liu, D.; Duncan, R. R. Rapid Formation of a Supramolecular Polypeptide-DNA Hydrogel for In Situ Three-Dimensional Multilayer Bioprinting. *Angew. Chem., Int. Ed.* **2015**, *54*, 3957−3961.
(63) Raeburn, J.; Mendoza-Cuenca, C.; Cattoz, B. N.; Little, M. A.; Terry, A. E.; Zamith Cardoso, A.; Griffiths, P. C.; Adams, D. J. The effect of solvent choice on the gelation and final hydrogel properties of Fmoc-diphenylalanine. *Soft Matter* **2015**, *11*, 927−935.
(64) Orbach, R.; Mironi-Harpaz, I.; Adler-Abramovich, L.; Mossou, E.; Mitchell, E. P.; Forsyth, V. T.; Gazit, E.; Seliktar, D. The Rheological and Structural Properties of Fmoc-Peptide-Based Hydrogels: The Effect of Aromatic Molecular Architecture of Self-Assembly and Physical Characteristics. *Langmuir* **2012**, *28*, 2015−2022.
(65) Brahms, S.; Brahms, J. Determination of Protein Secondary Structure in Solution by Vacuum Ultraviolet Circular Dichroism. *J. Mol. Biol.* **1980**, *138*, 149−178.
(66) Smith, A. M.; Williams, R. J.; Tang, C.; Coppo, P.; Collins, R. F.; Turner, M. L.; Saiani, A.; Ulijn, R. V. Fmoc-Dipenylalanine Self Assembles to a Hydrogel via a Novel Architecture Based on π-π Interlocked β-Sheets. *Adv. Mater.* **2008**, *20*, 37−41.
(67) Morris, K. L.; Chen, L.; Rodger, A.; Adams, D. J.; Serpell, L. C. Structural determinants in a library of low molecular weight gelators. *Soft Matter* **2015**, *11*, 1174−1181.
(68) Shih, W.-H.; Shih, W. Y.; Kim, S.-I.; Liu, J.; Aksay, I. A. *Phys. Rev. A: At., Mol., Opt. Phys.* **1990**, *42*, 4772−4779.
(69) Grant, M. C.; Russel, W. B. Volume-Fraction Dependence of Elastic Moduli and Transition Temperatures for Colloidal Silica Gels. *Phys. Rev. E: Stat. Phys., Plasmas, Fluids, Relat. Interdiscip. Top.* **1993**, *47* (4), 2606.
(70) Wu, H.; Morbidelli, M. A Model Relating Structure of Colloidal Gels to Their Elastic Properties. *Langmuir* **2001**, *17*, 1030−1036.
(71) Draper, E. R.; Morris, K. L.; Little, M. A.; Raeburn, J.; Colquhoun, C.; Cross, E. R.; McDonald, T. O.; Serpell, L. C.; Adams, D. J. Hydrogels formed from Fmoc amino acids. *CrystEngComm* **2015**, *17*, 8047.

DOI: 10.1021/acs.langmuir.5b02780
Langmuir 2015, 31, 12240−12250